Supporting Information for "Theoretical Predictions Suggest Carbon Dioxide Phases III and VII are Identical"

by W. Sontising, Y. Heit, J. McKinley, and G. Beran

Department of Chemistry, University of California, Riverside, California, 92521, USA.

Email: gregory.beran@ucr.edu

August 28, 2017

Contents

1 Comparison of predicted and experimental lattice parameters

Tables S1–S3 compare predicted lattice parameters against reported experimental structures. Selected predicted structures from the literature are included as well.

Matlab/GNU Octave scripts are provided separately which contain the quasi-harmonic room temperature HMBI MP2/CBS + AMOEBA structures for the pressures calculated explicitly and which can interpolate the structures at arbitrary pressures 1–20 GPa for phase I, and 0–60 GPa for phases II and III/VII. Because of the smooth variation in lattice parameters and fractional coordinates, interpolation reproduces the structures well.

Table S1: Comparison of predicted and experimental lattice parameters for phase I carbon dioxide ($Pa\bar{3}$ space group) at ambient temperature and selected pressures.

Method	Pressure	Temperature	a (Å)	Volume (cm^3/mol)	Source
Expt. (1998)	1 GPa	293 K	5.4942(2)	24.969(6)	Ref 1
MP2/CBS	1 GPa	296 K	5.504	25.11	this work
PBE-D3(BJ)[a]	1 GPa	n/a	5.515	27.59	Ref 2
Expt. (1994)	7.46 GPa	295 K	5.056(1)	19.46(2)	Ref 3
MP2/CBS	7.46 GPa	296 K	5.063	19.54	this work
Expt. (1994)	11.8 GPa	295 K	4.939(10)	18.14(11)	Ref 3
MP2/CBS	11.8 GPa	296 K	4.941	18.16	this work
MP2/aDZ[b]	11.8 GPa	n/a	4.91	17.82	Ref 4

[a] Thermal expansion was not included in the modeling.
[b] Using binary interaction model, without Counterpoise correction or thermal expansion.

Table S2: Comparison of predicted and experimental lattice parameters for phase II carbon dioxide ($P4_2/mnm$ space group).

Method	Pressure	Temperature	a (Å)	c (Å)	Volume (cm^3/mol)	$r_{C=O}$ (Å)	Source
Expt. (2002)	28 GPa	680 K	3.5345	4.1401	15.57	1.331(3)	Ref 5
MP2/CBS	28 GPa	680 K	3.504	4.125	15.25	1.155	this work
PBE-D3(BJ)[a]	28 GPa	n/a	3.51	4.06	15.09	1.157	Ref 2
Expt. (2014)	25.8 GPa	295 K	3.516(2)	4.104(2)	15.28	1.14	Ref 6
MP2/CBS	25.8 GPa	298 K	3.515	4.124	15.34	1.155	this work

[a] Thermal expansion was not included in the modeling.

Table S3: Comparison of predicted and experimental lattice parameters for phase III & VII carbon dioxide (*Cmca* space group).

Method	Pressure	Temperature	a (Å)	b (Å)	c (Å)	Volume (cm^3/mol)	Source
Expt. III	11.8 GPa	295 K	4.330(15)	4.657(5)	5.963(9)	18.11(8)	Ref 3
MP2/CBS	11.8 GPa	298 K	4.635	4.285	5.953	17.80	this work
MP2/aDZ[a]	11.8 GPa	n/a	4.63	4.33	5.80	17.82	Ref 4
PBE-D3(BJ)[b]	11.8 GPa	n/a	–	–	–	18.10	Ref 2
Expt. VII	12.1 GPa	726 K	4.746(1)	4.313(1)	5.948(1)	18.33	Ref 7
MP2/CBS	12.1 GPa	726 K	4.680	4.316	5.989	18.22	this work

[a] Using binary interaction model, without Counterpoise correction or thermal expansion.
[b] Thermal expansion was not included in the modeling; lattice parameters were not reported.

2 Equations of state

The P-V isotherms generated here were fitted to the Vinet equation of state (EOS),[8]

$$P = 3B_0 \frac{(1-\tilde{V})}{\tilde{V}^2} \exp\left[\frac{3}{2}(B_0' - 1)(1-\tilde{V})\right] \quad (1)$$

via non-linear least squares fitting to extract V_0, B_0, and B_0'. Here, $\tilde{V} = (V/V_0)^{1/3}$. As discussed in our earlier work,[9] fits using the Birch-Murnaghan EOS proved ill-constrained, with very different sets of V_0, B_0, and B_0' giving similar quality fits. The Vinet EOS behaves much better numerically in our experience, so it was used here instead.

Table S4 summarizes the equations of state obtained here and compares them against other theoretical and experimental values found in the literature. The agreement of quasiharmonic MP2 predictions for the bulk modulus of phase I has been discussed extensively previously.[9] The phase I bulk modulus decreases several fold between 0 K and room temperature. The B_0 obtained from quasi-harmonic MP2/CBS as a function of temperature is reasonable, as exemplified by the good agreement between it and the experimental data at room temperature shown here. Note that the bulk modulus reported by Yoo et al[5] appears to represent an unphysical fit, with a zero-pressure volume at room temperature that is smaller than even experimentally known volumes near 0 K.[9]

Other MP2 and dispersion-corrected density functional theory predictions that neglect thermal expansion typically obtain bulk modulus values that are several-fold larger than the room temperature value.[2,10] The PBE result of Bonev and co-workers[11] is fortuitously good, because the neglect of dispersion artificially makes the intermolecular interactions overly repulsive and expands the unit cell, which partially compensates for the neglected thermal expansion.

For phase II, the room-temperature MP2/CBS predictions are in reasonable agreement with the data PBE-D3 data of Gohr et al,[2] though the MP2 values are again slightly smaller (presumably due to neglect of thermal expansion in the PBE-D3 work). Again, PBE without dispersion produces a somewhat softer crystal that fortuitously agrees reasonably well with the MP2/CBS results. The MP2 predictions are in moderate agreement with the experimental results of Datchi and co-workers. As noted in that work, the lack of experimental low-pressure data for phase II introduces considerable uncertainty into their EOS fits. In contrast, the predicted B_0 of 131.5 from Yoo et al[5] is a clear outlier. The 18.0 cm^3/mol molar volume at zero pressure is only slightly larger than the 16.6 cm^3/mol volume at 20.6 GPa, in marked contrast to the predictions and the fit to Datchi.

For phase III, the three different sets of predict values are in reasonable agreement, with the PBE-D3 calculations that neglect thermal expansion again predicting a bulk modulus that is moderately larger, and the DFT calculations without dispersion predicting a cell that is too large and soft. Experimentally, only one value has been reported to our knowledge.[5] As with the phase I and II EOS data from the same study, the experimental phase III EOS data disagrees substantially from the calculations and suggests a material that is much harder (and similar to the bulk moduli of many metals). Given that all three phases I–III exhibit molecular crystalline structures, the much smaller bulk moduli predicted in three separate studies seem more likely to be correct.

Table S4: Summary of predicted and experimental room-temperature bulk modulus data for phases I–III. Literature data typically employed the Birch-Murnaghan EOS, while the fits in this work employed the Vinet EOS.

Method	Source	V_0 (cm^3/mol)	B_0 (GPa)	B_0'
Phase I				
PBE[a]	Bonev et al[11]	31.9	3.2	8.1
PBE-D3(BJD)[a]	Gohr et al[2]	27.6	9.9	5.4
MP2/aDZ[a,b]	Li et al[10]	23.7	16.1	6.9
MP2/aTZ[a,b]	Li et al[10]	24.5	12.1	7.7
MP2/CBS[a]	Heit et al[9]	24.6	10.6	7.8
MP2/CBS @ 296 K	Heit et al[9]	29.4	3.3	9.0
Experiment	Giordano et al 12	30.1±1	3±1	8.4±0.8
Experiment	Giordano et al[12c]	30.7±1	2±1	9±1
Experiment	Giordano et al[12d]	30.1±1	3±5	9±3
Experiment	Liu[13]	31.4	2.9	7.8
Experiment	Yoo et al[5]	25.1	6.2	6.2
Phase II				
PBE[a]	Bonev et al[11]	30.8	4.4	6.7
PBE-D3(BJD)[a]	Gohr et al[2]	27.6	7.5	6.3
MP2/CBS @ 298 K	this work	28.1	4.1	8.4
Experiment	Yoo et al[5]	18.0	131.5	2.1
Experiment	Datchi et al[6]	25±1	16±5	5.2±0.4
Experiment	Datchi et al[6]	26.7±0.2	8.5±0.3	6.3[e]
Phase III				
PBE[a]	Bonev et al[11]	33.0	3.53	7.12
PBE-D3(BJD)[a]	Gohr et al[2]	28.4	6.1	6.9
MP2/CBS @ 298 K	this work	28.0	4.6	5.5
Experiment	Yoo et al[5]	19.8	87	3.3

[a] No quasiharmonic approximation/finite temperature.
[b] No Counterpoise correction.
[c] Re-fit of Olinger data.[14]
[d] Re-fit of Liu data.[13]
[e] B_0' was fixed to Gohr PBE-D3(BJD) value.

3 Phase III optimization with fixed experimental cell

To investigate the claimed phase III structure, MP2/aug-cc-pVDZ optimization of the experimental phase III structure was performed with fixed lattice constants. As shown in Figure S1, the predicted structure agrees very well with the claimed experimental one, with an rmsd15 of 0.03 Å. For comparison, the rmsd15 between the experimental structures of phase III and VII is an order of magnitude larger at 0.24 Å. This phase III structure lies 4 kJ/mol above the fully relaxed phase VII-like structure, and it predicts a Raman spectrum that is appreciably different from the observed one (as discussed in the main paper).

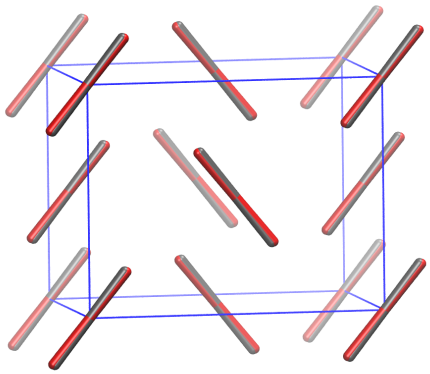

Figure S1: Comparison between the 11.8 GPa experimental phase III structure[3] (gray) and the MP2/aug-cc-pVDZ optimized one (red) when the optimization is performed with the experimental lattice parameters held fixed.

4 Impact of basis set on the predicted Raman spectra

In this study, Raman spectra were calculated at the MP2/aug-cc-pVDZ, albeit using frozen lattice parameters either optimized with quasiharmonic MP2/CBS or taken from experimentally reported crystal structures. MP2/aug-cc-pVDZ was used to relax the atomic positions within that fixed cell to a stationary point at the same level of theory and compute the phonon modes and Raman intensities. As shown in Figure S2, using the larger aug-cc-pVTZ basis to relax the atomic positions and compute the Raman spectra has only a modest impact on the predicted peak positions and intensities in the low-frequency region. For the phase I at 14.5 GPa and room temperature, it shifts the Raman-active lattice phonon modes down by 2% (2–6 cm^{-1}). These changes slightly improve agreement with experiment the T_{g-} and E_g modes, while making it slightly worse for the T_{g+} mode (see Figure S4 below).

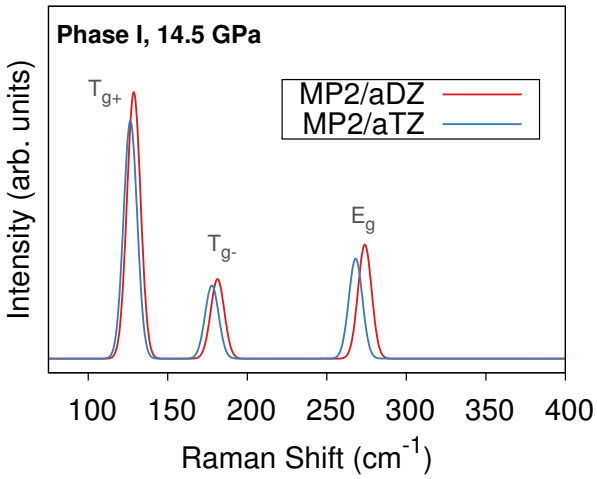

Figure S2: Comparison of the MP2/aug-cc-pVDZ and aug-cc-pVTZ predicted Raman spectra for phase I for the quasiharmonic MP2/CBS structure obtained at 14.5 GPa GPa and room temperature.

Use of full MP2/aug-cc-pVDZ optimization for phase IV: Though phase IV is not the focus of this study, Figure 4a in the main paper presents Raman spectra for phase IV that were fully optimized (both lattice parameters and atomic positions) at the MP2/aug-cc-pVDZ level. While this approach is not expected to be as accurate as the MP2/CBS quasiharmonic calculations for determining the lattice parameters, it actually performs better than one might expect due to fortuitous error cancellation between the underbinding of the crystal at the MP2/aug-cc-pVDZ level and the neglect of thermal expansion. The former overestimates the cell volume, while the latter underestimates it. Detailed analysis of basis set and thermal expansion for phase I has been reported previously.[9] As shown in Figure S3, this inexpensive approximation performs reasonably. Other examples of the performance of this approximation in carbon dioxide can be found in Refs 4 and 10.

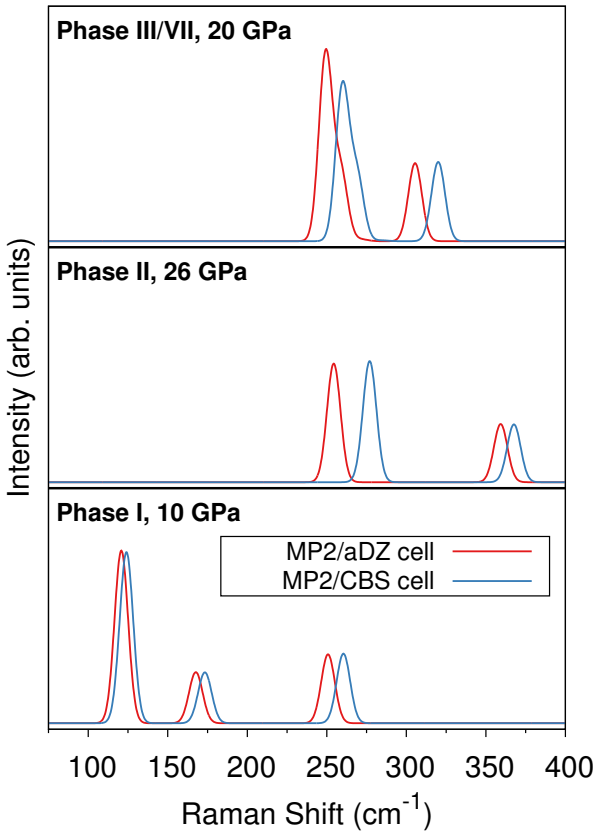

Figure S3: Comparison of predicted MP2/aug-cc-pVDZ Raman spectra when the cell is fully optimized with MP2/aug-cc-pVDZ (and no quasiharmonic approximation) instead of using the quasiharmonic MP2/CBS lattice parameters for three different examples.

5 Pressure dependence of the Raman spectra

Phase I: Figure S4a compares our predicted MP2/aug-cc-pVDZ Raman shift frequencies from the quasiharmonic approximation (QHA) MP2/CBS unit cells against experiment[12] at room temperature as a function of pressure for phase I. Figure S4b reports MP2/aug-cc-pVDZ results from Li et al[4] which employ a slightly different fragment approach. The calculations of Li et al optimized the unit cell at the MP2/aug-cc-pVDZ level instead of MP2/CBS, and no quasi-harmonic approximation was employed. Comparison of Figures S4a and S4b indicate that the simpler model used by Li et al works well at higher pressure, but it performs worse at lower pressures where thermal expansion is more significant. Figure S4c plots the PBE density functional theory (DFT) results from Bonev et al.[11] Those results are also in generally good agreement with experiment. However, those 2003 results did not employ a dispersion correction, which leads to artificial expansion of the unit cell. This is observed in the systematic underestimation of the prediction phonon frequencies.

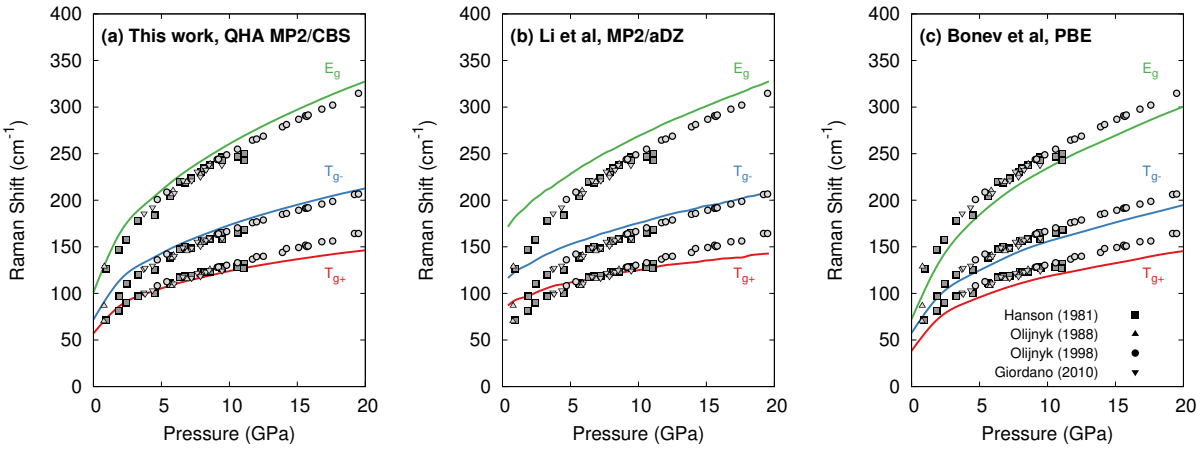

Figure S4: Pressure dependence of the librational Raman modes for phase I at room temperature. Comparison of MP2/aug-cc-pVDZ predictions based on quasiharmonic MP2/CBS structures from this work, results entirely at the MP2/aug-cc-pVDZ level with no quasiharmonic approximation from Li et al,[4] and PBE DFT results from Bonev et al.[11] Points indicate experimental data,[12,15–17] while lines correspond to the predicted frequencies.

Phase II: Experimental pressure-dependent Raman data for phase II largely comes from Iota et al (2001).[18] At the time, the structure of phase II was unclear, and the low-frequency Raman spectrum was fitted to three distinct modes, with highest-frequency mode ("mode C" in Ref 18) fitted to the shoulder of the experimentally observed peak that is now attributed to the B_{1g} mode. Subsequent data from Yoo et al (2002)[5] and Datchi et al (2014)[6] fitted to only two distinct modes (B_{1g} and E_g) as expected from the space group and confirmed by theoretical calculations here and from Bonev et al.[11]

Ignoring the spurious "mode C", the agreement between theory and experiment is fairly good across the pressure range for both the MP2 calculations reported here and the earlier DFT ones from Bonev et al.[11]

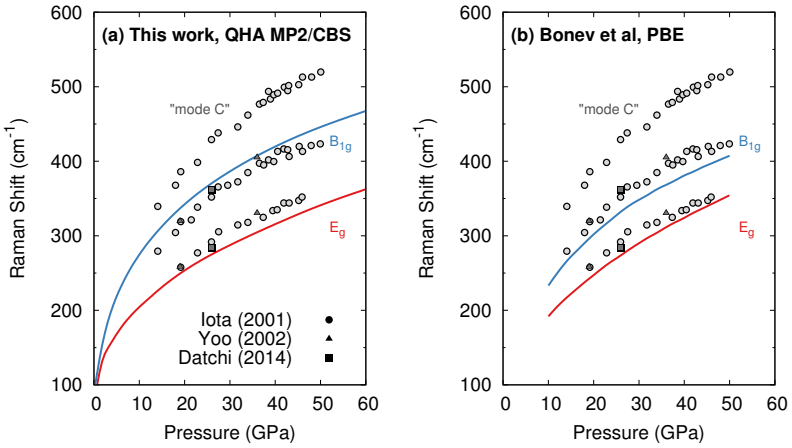

Figure S5: Pressure dependence of the librational Raman modes for phase II at room temperature. Comparison of MP2/aug-cc-pVDZ predictions based on quasiharmonic MP2/CBS structures from this work and PBE DFT from Bonev et al[11] (lines) against experimental data (points).[5,6,18]

Phase III/VII: Figure S6 compares pressure dependent experimental Raman study of Olijnyk and Jephcoat[17] against MP2 predictions from this work and PBE DFT calculations by Bonev et al.[11] Note that Li et al[4] also predicted phase III phonons as a function of pressure, though they are not included here because the symmetry character of the mode assignments in Figure 6 of Li et al is not clear. Nevertheless, the Raman plot in Figure 5 of Li et al shows three larger peaks and one very weak one around 300 cm^{-1} at 18 GPa, which is generally consistent with our predictions.

Although Bonev et al did not report Raman intensities, the mode symmetries follow the same pattern in both the MP2 and PBE results. At low pressure, the modes are, in order of increasing frequency: A_g, B_{1g}, B_{3g}, and B_{2g}. Around 25–30 GPa, the A_g and B_{1g} modes cross. Experimentally, the lowest-frequency mode (mode a in the main paper) is difficult to observe after 20 GPa.[17] The two middle experimental modes (b and c in the main paper) cross around 25 GPa, just as for the predicted A_g and B_{1g} modes. Finally, the highest-frequency experimental mode (d in the main paper) agrees well with the B_{2g} mode predicted here. As discussed in the main paper, we hypothesize that the lowest-frequency experimental mode is artifactual, and the fourth expected librational mode is actually the low-intensity B_{3g} mode. Because of the lack of dispersion in the Bonev calculations the phonon modes are artificially shifted to lower frequencies, giving a nominal appearance of agreement with the experimental assignment. However, we believe the symmetry character and crossing behavior of the modes is more consistent with the MP2 predictions in the current study. Repeating the DFT calculations with a dispersion-correction theory would likely shift the modes to higher frequencies, in better agreement with our MP2 predictions.

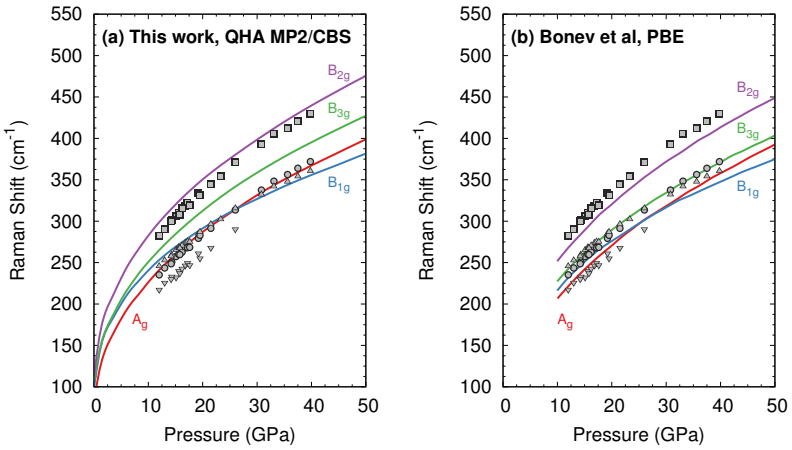

Figure S6: Pressure dependence of the librational Raman modes for phase III at room temperature. Comparison of MP2/aug-cc-pVDZ predictions based on quasiharmonic MP2/CBS structures from this work and PBE DFT results from Bonev et al[11] (lines) against experimental data from Olijnyk and Jephcoat (points).[17]

6 Crystal structure prediction results

Crystal structure prediction was performed using USPEX to generate potential candidate structures which might better account for phase III. As described in the main text, evolutionary algorithms were employed to generate more than 1700 structures, though large numbers of these were duplicates or energetically unfavorable. The 91 lowest structures were relaxed with PBE-D2 under 11.8 GPa of pressure, and many additional structures either coalesced into a single structure or proved energetically unfavorable. In the end, 25 structures had enthalpies within 10 kJ/mol of the most stable one (phase II) at this pressure, as shown in Figure 5a of the main paper. Figure S7 plots simulated powder X-ray diffraction (PXRD) patterns for all 25 structures. The crystal structure prediction generated phase I, II, and VII structures. It did not generate phase IV, which has a larger number of molecules in the unit cell.

The PXRD experiment was performed on a sample believed to consist of a mixture of phase I and III.[3] Examination of all the patterns reveals that none of the structures which are not experimentally known provides a good match to the experimental PXRD. The best matches come from either the claimed phase III structure or the phase VII one (with some mixture of phase I). CIF Structure files for all 25 structures are provided separately.

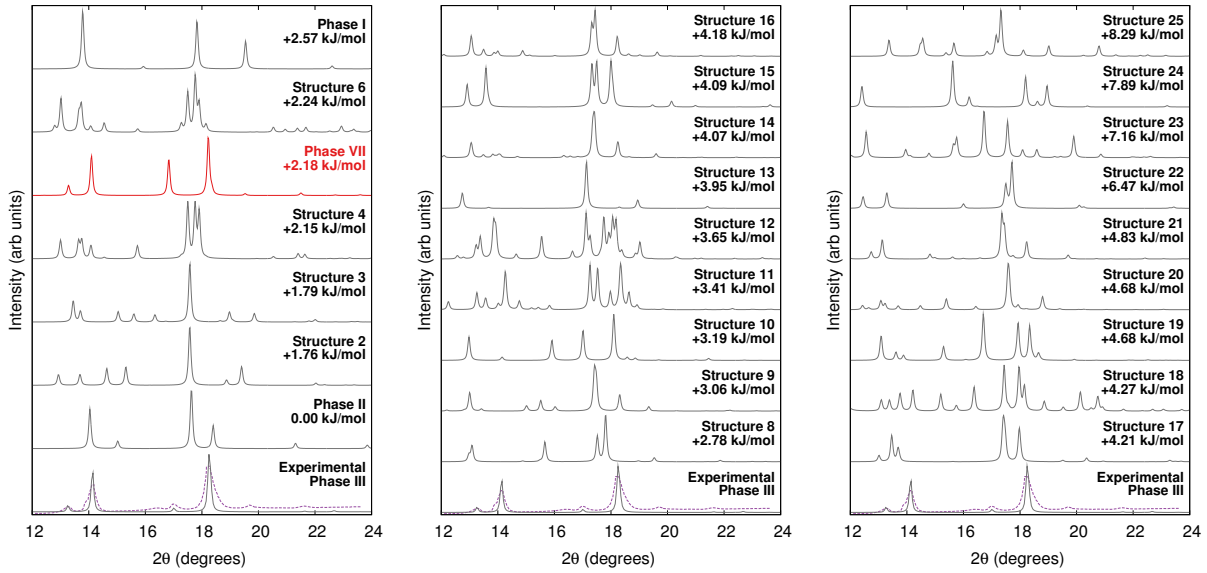

Figure S7: Simulated powder X-ray diffraction patterns for the 25 predicted crystal structures which lie within 10 kJ/mol of the stable phase II one. All were optimized at the PBE-D2 level and 11.8 GPa, including those identified as Phase I, II, or VII. These patterns are compared against the actual experimental phase III powder X-ray diffraction pattern (purple dotted line) and the simulated phase III spectrum based on the claimed experimental structure.[3]

References

[1] R. T. Downs and M. S. Somayazulu, Acta Cryst. C **54**, 897 (1998).
[2] S. Gohr, S. Grimme, T. Söhnel, B. Paulus, and P. Schwerdtfeger, J. Chem. Phys. **139**, 174501 (2013).
[3] K. Aoki, H. Yamawaki, M. Sakashita, Y. Gotoh, and K. Takemura, Science **263**, 356 (1994).
[4] J. Li, O. Sode, G. A. Voth, and S. Hirata, Nature Commun. **4**, 2647 (2013).
[5] C. Yoo, H. Kohlmann, H. Cynn, M. Nicol, V. Iota, and T. LeBihan, Phys. Rev. B **65**, 1 (2002).
[6] F. Datchi, B. Mallick, A. Salamat, G. Rousse, S. Ninet, G. Garbarino, P. Bouvier, and M. Mezouar, Phys. Rev. B **89**, 144101 (2014).
[7] V. M. Giordano and F. Datchi, Europhys. Lett. **77**, 46002 (2007).
[8] P. Vinet, J. R. Smith, J. Ferrante, and J. H. Rose, Phys. Rev. B **35**, 1945 (1987).
[9] Y. N. Heit, K. D. Nanda, and G. J. O. Beran, Chem. Sci. **7**, 246 (2016).
[10] J. Li, O. Sode, and S. Hirata, J. Chem. Theory Comput. **11**, 224 (2015).
[11] S. A. Bonev, F. Gygi, T. Ogitsu, and G. Galli, Phys. Rev. Lett. **91**, 065501 (2003).
[12] V. M. Giordano, F. Datchi, F. A. Gorelli, and R. Bini, J. Chem. Phys. **133**, 144501 (2010).
[13] L. Liu, Earth Planet. Sci. Lett. **71**, 104 (1984).
[14] B. Olinger, J. Chem. Phys. **77**, 6255 (1982).
[15] R. C. Hanson and L. H. Jones, J. Chem. Phys. **75**, 1102 (1981).
[16] H. Olijnyk, H. Däufer, H.-J. Jodl, and H. D. Hochheimer, J. Chem. Phys. **88**, 4204 (1988).
[17] H. Olijnyk and A. P. Jephcoat, Phys. Rev. B **57**, 879 (1998).
[18] V. Iota and C. S. Yoo, Phys. Rev. Lett. **86**, 5922 (2001).